The switch complex ArlCDE connects the chemotaxis system and the archaellum

Li, Zhengqun; Rodriguez-Franco, Marta; Albers, Sonja Verena; Quax, Tessa E. F.

IMPORTANT NOTE: You are advised to consult the publisher's version (publisher's PDF) if you wish to cite from it. Please check the document version below.

Document Version
Publisher's PDF, also known as Version of record

Publication date:
2020

[Link to publication in University of Groningen/UMCG research database](#)

RESEARCH ARTICLE

WILEY

The switch complex ArlCDE connects the chemotaxis system and the archaellum

Zhengqun Li[1] | Marta Rodriguez-Franco[2] | Sonja-Verena Albers [ID] [1] | Tessa E. F. Quax [ID] [3]

[1]Molecular Biology of Archaea, Faculty of Biology, University of Freiburg, Freiburg, Germany

[2]Cell Biology, Faculty of Biology, University of Freiburg, Freiburg, Germany

[3]Archaeal Virus–Host Interactions, Faculty of Biology, University of Freiburg, Freiburg, Germany

Correspondence
Sonja-Verena Albers, Molecular Biology of Archaea, Faculty of Biology, University of Freiburg, Freiburg, Germany.
Email: sonja.albers@biologie.uni-freiburg.de

Tessa E. F. Quax, Archaeal Virus–Host Interactions, Faculty of Biology, University of Freiburg, Freiburg, Germany.
Email: tessa.quax@biologie.uni-freiburg.de

Funding information
Deutsche Forschungsgemeinschaft, Grant/Award Number: 403222702-SFB 1381 and 411069969; China Scholarship Council

Abstract

Cells require a sensory system and a motility structure to achieve directed movement. Bacteria and archaea possess rotating filamentous motility structures that work in concert with the sensory chemotaxis system. This allows microorganisms to move along chemical gradients. The central response regulator protein CheY can bind to the motor of the motility structure, the flagellum in bacteria, and the archaellum in archaea. Both motility structures have a fundamentally different protein composition and structural organization. Yet, both systems receive input from the chemotaxis system. So far, it was unknown how the signal is transferred from the archaeal CheY to the archaellum motor to initiate motor switching. We applied a fluorescent microscopy approach in the model euryarchaeon *Haloferax volcanii* and shed light on the sequence order in which signals are transferred from the chemotaxis system to the archaellum. Our findings indicate that the euryarchaeal-specific ArlCDE are part of the archaellum motor and that they directly receive input from the chemotaxis system via the adaptor protein CheF. Hence, ArlCDE are an important feature of the archaellum of euryarchaea, are essential for signal transduction during chemotaxis and represent the archaeal switch complex.

KEYWORDS
archaea, archaeal flagellum, archaellum, chemosensory arrays, chemotaxis, motility

1 | INTRODUCTION

Bacteria and archaea employ rotating filamentous structures to swim through liquid environments. Although they are functionally similar, there is no structural similarity between the filaments from bacteria and archaea (Berg and Anderson, 1973; Alam and Oesterhelt, 1984; Chevance and Hughes, 2008; Jarrell and Albers, 2012; Albers and Jarrell, 2018; Beeby *et al.*, 2020). The archaeal motility structure, the archaellum, has homology to bacterial type IV pili, and it consists of ~10 different Arl proteins (previously named Fla proteins) (Kalmokoff and Jarrell, 1991; Jarrell and Albers, 2012; Pohlschroder *et al.*, 2018).

The energy required for the rotation is derived from ATP hydrolysis (Thomas *et al.*, 2002; Streif *et al.*, 2008; Reindl *et al.*, 2013) and new protein subunits are N-terminally processed and added at the base of the growing filament (Kalmokoff and Jarrell, 1991; Bardy and Jarrell, 2003; Szabo *et al.*, 2006). In contrast, the bacterial motility structure, the flagellum, consists of over 30 different proteins, which are not found in archaea (Chevance and Hughes, 2008; Erhardt *et al.*, 2010; Lassak *et al.*, 2012; Altegoer and Bange, 2015). The energy for flagellum rotation originates from the proton motive force and new protein subunits are added at the tip of the growing filament (Chevance and Hughes, 2008; Erhardt *et al.*, 2010; Altegoer and Bange, 2015).

Despite the fundamental differences in the organization of the archaeal and bacterial motility structures, archaea and bacteria both possess the chemotaxis system (Marwan *et al*., 1991; Briegel *et al*., 2015; Quax *et al*., 2018a). This system allows cells to move along chemical gradients and, in combination with the motility structure, ensures directional movement (Szurmant and Ordal, 2004; Porter *et al*., 2011; Bi and Sourjik, 2018). Archaea, such as euryarchaea and some thaumarchaea, have likely received the chemotaxis system from bacteria via horizontal gene transfer (Wuichet *et al*., 2010; Wuichet and Zhulin, 2010; Briegel *et al*., 2015).

In bacteria, the chemotaxis system transfers signals to the base of the flagellum (Sourjik and Berg, 2002; Chevance and Hughes, 2008). Attractants or repellents can bind to chemosensory receptors, methyl-accepting chemotaxis proteins (MCPs), which are often present at the cell surface (Parkinson *et al*., 2015; Salah Ud-Din and Roujeinikova, 2017). These MCPs are organized together with CheW and CheA proteins in chemosensory arrays, which are large organized clusters that ensure signal integration and amplification (Briegel *et al*., 2012; 2014). Binding of stimuli to the MCPs triggers a signaling cascade, which eventually leads to the phosphorylation of the response regulator protein CheY (Welch *et al*., 1993; Parkinson *et al*., 2015). Phosphorylated CheY binds with higher affinity to the "switch complex" at the base of the flagellum motor, which consists of FliM, FliN, and FliG proteins (Barak and Eisenbach, 1992; Sarkar *et al*., 2010; Paul *et al*., 2011). This results in a change or a pause in the flagellum rotation direction (Sarkar *et al*., 2010; Paul *et al*., 2011). As archaea lack homologs of the switch complex (Jarrell and Albers, 2012), we searched for archaellum motor proteins receiving signals from the chemotaxis system.

Recently available cryo-EM structures of the archaellum provide clues to this question. Sub-tomogram averaging of the archaellum motor of the euryarchaeon *Pyrococcus furiosus* revealed a bell-like structure below the motor that stretches into the cytoplasm (Daum *et al*., 2017). The central core of the motor is formed by the proteins ArlJ, ArlI, and ArlH (previously named FlaJ, I and H) encoded by the archaellum operon (Figure 1a) (Ghosh *et al*., 2011; Banerjee *et al*., 2013; Reindl *et al*., 2013; Chaudhury *et al*., 2016; 2018; Albers and Jarrell, 2018). ArlJ is an integral membrane protein that was not well resolved in the cryo-Em structure (Daum *et al*., 2014). Six copies of the cytosolic ATPase ArlI and six of the ATP binding protein ArlH, could be mapped into the cytosolic part of the central core of the archaellum (Daum *et al*., 2017). After mapping ArlI and ArlH, still a large proportion of the cytosolic part of the motor has remained unassigned (Daum *et al*., 2017). This density has a ring-like shape and was hypothesized to be occupied by ArlC, D, and E, because these are the only proteins with unassigned function encoded in eurayarchaeal archaellum operons (Figure 1a). It was suggested that these proteins together form a ring structure, in analogy to the ring structure formed by the crenarchaeal-specific protein ArlX protein (Daum *et al*., 2017; Briegel *et al*., 2017). Euryarchaea encode ArlCDE, while Crenarchaea lack these proteins and instead possess the

motor protein ArlX (Jarrell and Albers, 2012). In many euryarchaeal genomes, different combinations of fusions of ArlC, D, and E are encoded, such as ArlCE from the halophilic euryarchaeon *Haloferax volcanii*, which suggests that the three proteins might form a complex (Albers and Jarrell, 2015). Since the unassigned ring-like density is at the most peripheral part of the motor, it would represent a convenient docking place for chemotaxis proteins. Corresponding with this hypothesis, an interactome study in *Halobacterium salinarum*, previously indicated that ArlCE (fused in this organism) interacts with the archaeal-specific chemotaxis protein CheF (Figure 1a) (Schlesner *et al*., 2009; 2012). Motile archaea encoding the bacterial-like chemotaxis system, all possess the adaptor protein CheF, which can bind to CheY and as such forms a link between the chemotaxis system and archaellum (Schlesner *et al*., 2009; Quax *et al*., 2018b; Paithankar *et al*., 2019). CheF possesses a DUF439 domain of the unknown function and is exclusively present in chemotaxis operons of archaea and it is not found in bacteria (Schlesner *et al*., 2009). Phosphorylation of archaeal CheY is stimulating binding to CheF and the phosphorylation site is important for the CheY function (Quax *et al*., 2018b).

We aimed to establish in which sequence order chemotaxis proteins transfer signals to the archaellum motor and which motor proteins are likely in direct contact with the chemotaxis system. To address these questions, we used *H. volcanii*, for which a well-developed genetic manipulation system is available, in addition to previously obtained information on the cellular positioning of several chemotaxis and archaellum proteins (Allers *et al*., 2004; Li *et al*., 2019). Fluorescent microscopy was employed to study the localization of several proteins, important for signal transduction between the chemotaxis system and the motility machinery. This work sheds light on the role of the ArlC, D, and E archaellum proteins and indicates that they are a crucial factor in receiving the input from the chemotaxis system.

2 | RESULTS

2.1 | The chemosensory arrays anchor the archaeal response regulator CheY

We aimed to gain insight into the sequence in which archaeal chemotaxis and archaellum proteins are interacting with each other. First, we focused on the response regulator CheY, which is thought to shuttle between the chemotaxis system and the motility structure (Figure 1a). Previously, we have shown that CheY localizes primarily to the cell poles of motile cells, but it is also present at the lateral membranes (Li *et al*., 2019). This positioning pattern shares similarities with that of the chemosensory arrays and with that of archaella, which are exclusively present at cell poles (Li *et al*., 2019). As CheY was shown to interact with the archaeal-specific chemotaxis protein CheF (Schlesner *et al*., 2009; Quax *et al*., 2018b), we wondered if it might position at the archaellum motor in a CheF dependent manner. *H. volcanii* encodes two CheF homologs. CheF2 is conserved in
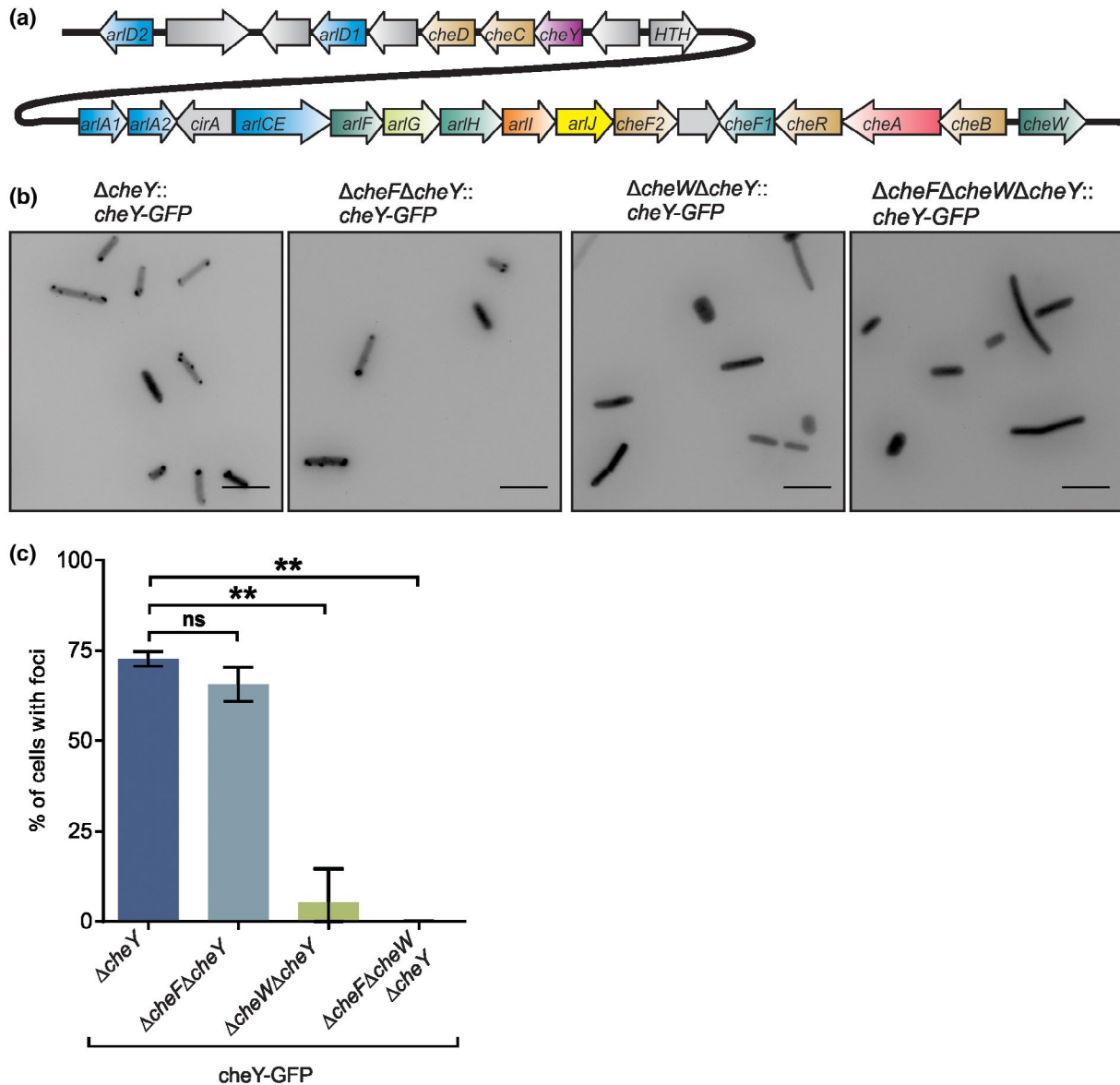
FIGURE 1 Intracellular positioning of CheY is mainly dependent on chemosensory arrays in *H. volcanii*. (a) Schematic representation of the archaellum and chemotaxis operon in the model euryarchaeal *H. volcanii* (b) Representative fluorescent micrographs of the intracellular distribution of CheY-GFP clusters in different *H. volcanii* mutants in early stationary phase. I, Δ*cheY*; II, Δ*cheF* Δ*cheY*; III, Δ*cheW* Δ*cheY*; IV, Δ*cheF* Δ*cheW* Δ*cheY*. The number of cells analyzed for each mutant is *n* > 500. Scale bars, 5 μm. (c) Percentages of cells with CheY-GFP foci in the four strains analyzed in (a). ** *p* < .01. ns, not significant *p* > .05

all archaea with a chemotaxis system, while CheF2 is more specific for haloarchaea (Schlesner *et al.*, 2009). In addition, it was shown that only CheF1 is important for directional movement (Quax *et al.*, 2018b). This protein will be further referred to as CheF. A *H. volcanii* Δ*cheY* Δ*cheF* mutant was constructed in which either CheY-GFP or GFP-CheF were expressed. These fusion proteins were shown to be correctly expressed by Western blot analysis and were previously shown to restore motility on semi-solid agar plates (Figure S1a. Table S1) (Li *et al.*, 2019). The positioning pattern of GFP-CheY did not significantly differ in the Δ*cheY*Δ*cheF* and in the Δ*cheY* strain (Figure 1b,c). In both cases, polar and lateral foci were observed, suggesting that he localization of the response regulator CheY is mainly independent of CheF (Figure 1b,c).

Next, we tested if CheY might bind to chemosensory arrays. CheW is a small adaptor protein, which together with the MCPs and CheA builds chemosensory arrays (Griswold *et al.*, 2002; Li *et al.*, 2013; Briegel *et al.*, 2014). CheW was previously used as a marker protein to indicate the cellular position of chemosensory arrays in *H. volcanii* (Li *et al.*, 2019). A Δ*cheY* Δ*cheW* deletion strain was created in which CheY-GFP was expressed. Observation of this strain by fluorescent microscopy showed that cells mostly displayed a diffuse fluorescent signal in the cytoplasm, with the exception of a few polar foci in a low number of cells (5.3%) (Figure 1b,c). When GFP-CheY was expressed in a Δ*cheY*Δ*cheF*Δ*cheW* strain, also the residual signal at the cell poles disappeared and the fluorescent signal was exclusively diffuse (Figure 1b,c). These findings indicate that in

exponentially growing cells, CheY is mainly bound to chemosensory arrays, while a very small fraction might be present at the archaellum motor via binding to CheF.

2.2 | ArlD and ArlCE are important for communication with the chemotaxis system

CheF was previously shown to position mainly at the cell poles of *H. volcanii* (Li *et al.*, 2019). Therefore, we asked if CheF could be permanently localized at the archaellum motor in motile cells. The proteins ArlD and ArlCE are encoded in the archaellum operon in euryarchaea and have an unknown function (Figure 1a) (Albers and Jarrell, 2015; 2018). They are hypothesized to be part of the archaellum motor (Briegel *et al.*, 2017; Daum *et al.*, 2017) and preliminary data from *M. maripaludis* suggest that they are membrane associated, although they both lack a transmembrane domain (Thomas and Jarrell, 2001; Thomas *et al.*, 2002). As an interactome study suggested that ArlCE might be in direct contact with the archaeal-specific chemotaxis protein CheF (Schlesner *et al.*, 2009), we asked if CheF requires ArlCE and ArlD to bind to the archaellum motor. As *H. volcanii* encodes two ArlD homologs (with 35% amino acid sequence identity), we made knock-outs of both genes. *arlD2* is encoded from a gene a little upstream of the archaellum operon (Figure 1a). Analysis of a Δ*arlD2* strain on the semi-solid agar plate showed that directional movement and motility were comparable to the wild type (Figure S2a,b). In contrast, Δ*arlD1* has a severe motility defect, as the archaellum is not correctly produced anymore (Li *et al.*, 2019). Therefore, we continued with ArlD1 and refer to this protein as ArlD, throughout the paper. Next, we constructed the Δ*arlD* Δ*cheF* and Δ*arlCE* Δ*cheF* deletion strains in *H. volcanii*. GFP-CheF was expressed in Δ*arlD* Δ*cheF* and Δ*arlCE* Δ*cheF*. Interestingly, the positioning pattern of GFP-CheF showed a significant difference in both Δ*arlD* Δ*cheF* and Δ*arlCE* Δ*cheF* strain compared to that in a Δ*cheF* strain (Figure 2a,b). GFP-CheF foci were observed at the cell poles in 65% of Δ*cheF* cells, consistent with what has been described previously (Table S1) (Li *et al.*, 2019). In contrast, the number of cells with polar GFP-CheF foci was significantly reduced in both Δ*arlD* Δ*cheF* and Δ*arlCE* Δ*cheF* strain (to ~20% of cells) (Figure 2a,b). These findings indicate that ArlD and ArlCE promote, but are not essential for, CheF positioning to the cell pole. It might be possible that the largest fraction of CheF proteins is positioned at the cell pole via interaction with ArlCE and ArlD that are bound to the archaellum motor. A smaller fraction of CheF might be positioned at the cell pole because of other protein interactions.

2.3 | Polar positioning of ArlD and ArlCE is interdependent

After we demonstrated the importance of ArlD and ArlCE for positioning of the chemotaxis adaptor protein CheF, we aimed to gain more information on the possible function of these two proteins.
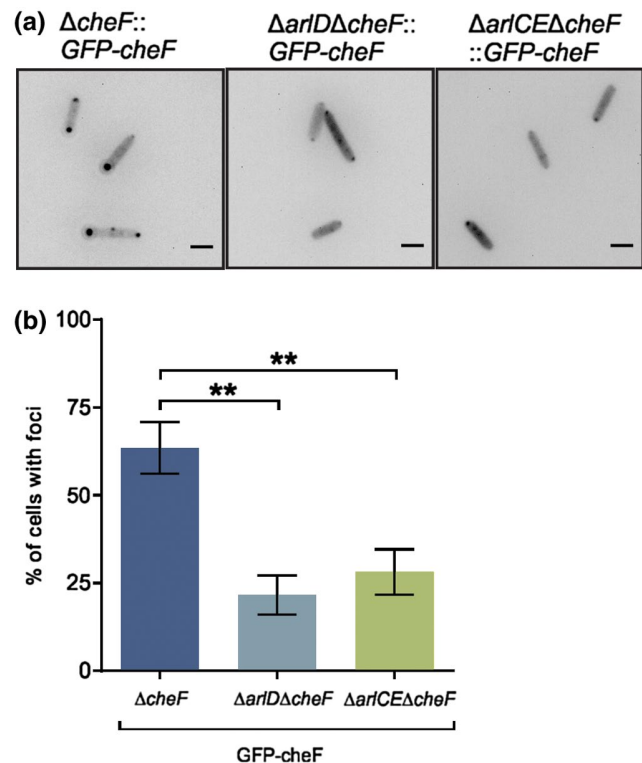

FIGURE 2 The archaellum proteins ArlD and ArlCE are important for communication with the chemotaxis system. (a) Representative fluorescent images of the intracellular distribution of GFP-CheF clusters in different *H. volcanii* mutants in exponential phase Scale bars, 2 μm. (b) Percentages of cells with GFP-CheF clusters in the strains described in (a). The number of cells of each mutant analyzed is *n* > 500. ******p* < .01 as established by *t* test

Previously we have shown that ArlD is likely part of the archaellum motor, as fluorescent fusion proteins of ArlD were positioned at the cell poles of rod-shaped motile *H. volcanii* cells, the location where also archaella are found (Table S1) (Li *et al.*, 2019). In order to test if the ArlCE protein is also part of the archaellum motor, we constructed a Δ*arlCE* deletion strain. Analysis by EM showed that this strain does not have archaella at its surface (Figure 3a) and did not form motility rings on the semi-solid agar plate (Figure 3b). We expressed N- and C-terminal GFP fusions of ArlCE in a Δ*arlCE* strain. While the expression of native ArlCE could restore the motile phenotype on the semi-solid agar plate (Figure 3b), both GFP fusions did not restore motility (Table S1). Western blot analysis with α-GFP antibodies did not show a clear signal for either fusion, indicating that the expression of ArlCE fusions to GFP yielded only low levels of the fusion proteins (data not shown). Correspondingly, Δ*arlCE* strains expressing GFP-ArlCE or ArlCE-GFP observed by fluorescence microscopy had only a very low total GFP signal. Still, distinct foci were observed, exclusively near the cell poles of the motile rod-shaped cells (Figure 3c). About 39% of the cells showed an ArlCE-GFP signal at one pole, while 42% showed bipolar ArlCE-GFP foci. The percentages were similar to the GFP-ArlCE signals. This positioning pattern is reminiscent of that of ArlD, suggesting that ArlCE also positions at the archaellum motor (Li *et al.*, 2019).
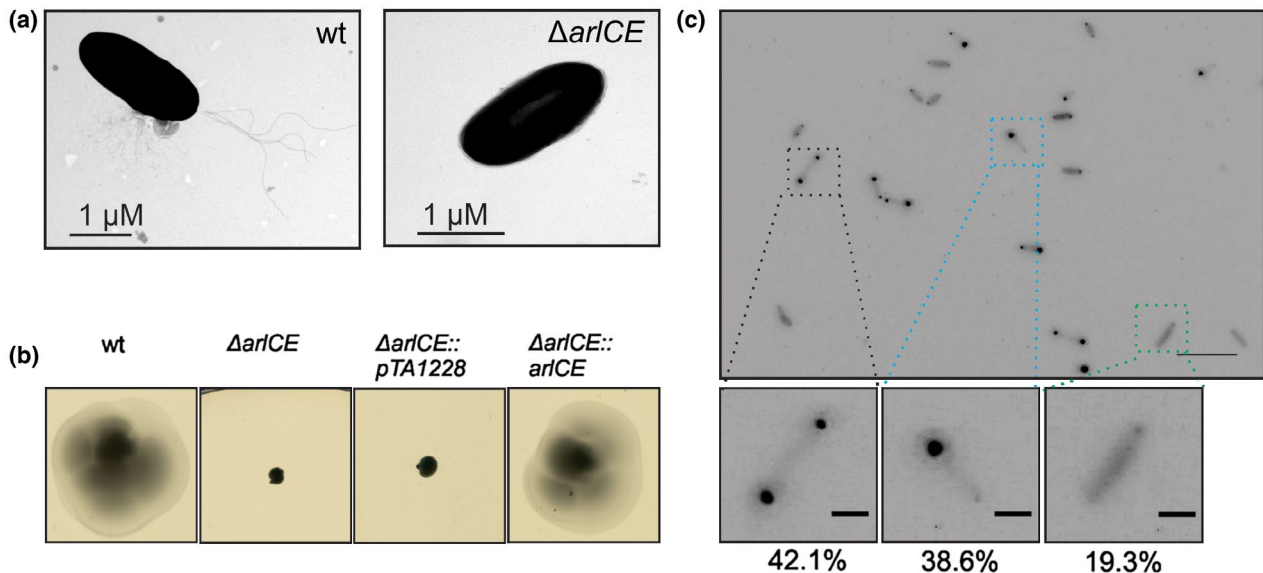
FIGURE 3 The positioning pattern of ArlCE is reminiscent of that of ArlD. (a) Transmission electron microscopy (TEM) of the wild-type (WT) and ΔarlCE *H. volcanii* cells. Scale bar, 1 μm. (b) Influence of ArlCE on directional movement. Representative image of motility assay of different *H. volcanii* strains on semis solid agar plates. This experiment was performed on at least three independent occasions. pTA1228, empty plasmid (c) Representative fluorescent image of ArlCE-GFP clusters in *H. volcanii* ΔarlCE cells in the early exponential phase. The percentages of cells with each positioning pattern are shown below the corresponding exemplary images. The total population of the analyzed cells was *n* > 500. Scale bars, 10 μm (upper panel) and 2 μm (lower panels)

To confirm this hypothesis, ArlD-GFP and ArlCE-mCherry were co-expressed in a ΔarlD ΔarlCE strain. The signals of both proteins overlapped, suggesting that ArlD and ArlCE co-localized in the cell (Figure 4a). To study if the positioning of the two proteins was interdependent, ArlD-GFP or ArlCE-GFP were expressed in the ΔarlCE ΔarlD strain. Western blot analysis showed that ArlD-GFP was correctly expressed in this background (Figure S1c). Comparison with the positioning pattern of the two proteins in the control strains showed that the number of cells with distinct ArlD or ArlCE foci was significantly reduced in the absence of either of the other protein (Figures 4b, S2c). Thus, the correct positioning of ArlD or ArlCE at the archaellum motor is dependent on the presence of both proteins. This suggests that ArlD and ArlCE might form a precomplex, required for binding to the archaellum motor.

ArlD and ArlCE promote the positioning of CheF at the cell pole (Figure 2). To test if ArlD and ArlCE also require CheF for polar localization, we expressed ArlD-GFP and ArlCE-GFP in ΔarlD ΔcheF strain and ΔarlCE ΔcheF strain, respectively. We compared the number of cells with polar foci in these strains with those of ΔarlD ArlD-GFP and ΔarlCE ArlCE-GFP strain. The positioning pattern of ArlD and ArlCE was not significantly affected by the absence of CheF (Figure S3). Thus, ArlD and ArlCE do not require CheF for correct positioning at the cell pole.

2.4 | ArlD and ArlCE dock on the archaellum motor via binding to ArlH

As we demonstrated that CheF is not responsible for polar positioning of ArlCE and ArlD, we hypothesized that the ArlCE and
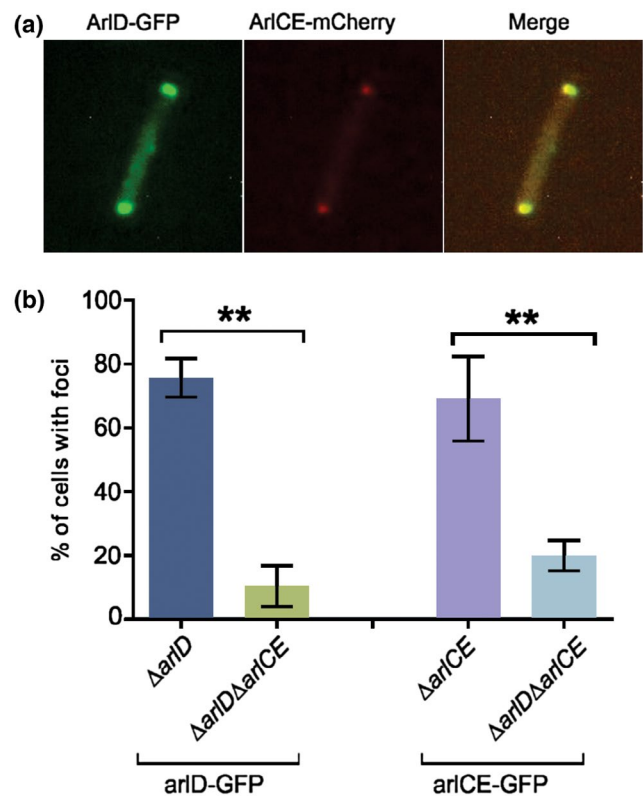

FIGURE 4 The positioning of ArlD and ArlCE are dependent on each other in *H. volcanii*. (a) Co-expression of ArlD-GFP and ArlCE-mCherry in the *H. volcanii* ΔarlD ΔarlCE strain in early exponential phase. (b) Percentages of cells with intracellular ArlD or ArlCE foci in single and double knockout strains. *N* > 500. **p < .01 as established by *t* test

ArlD proteins are likely localized at the cell pole by direct binding to the archaellum motor. The core of the motor consists of ArlH, ArlI and the membrane protein ArlJ, which interact with each other to form a large oligomeric complex (Banerjee *et al.*, 2013; Reindl *et al.*, 2013; Chaudhury *et al.*, 2016). The cryo-EM structure of the archaellum motor of euryarchaea was resolved previously, which indicated that ArlH interacts with a ring-like density that might consist of ArlC, D, and E (Daum *et al.*, 2017). Therefore, we first tested if ArlD and ArlCE might require ArlH for polar localization. First, a ΔarlH strain was constructed in *H. volcanii*. Analysis on the semi-solid agar plate showed that the ΔarlH strain did not form motility rings, in correspondence with the fact that a mutant in other archaea was previously shown to possess no archaella (Chaban *et al.*, 2007; Staudinger, 2008; Chaudhury *et al.*, 2016) (Figure 5a). Expression of native ArlH in the ΔarlH strain could complement

the ability of motility on the semi-solid agar plate (Figure 5a). In contrast, expression of an ArlH-GFP fusion did not restore motility (Table S1). However, Western blot analysis indicated that the fusion protein ArlH-GFP was correctly expressed (Figure S1b) and expression of ArlH-GFP in the ΔarlH strain resulted in foci at the cell pole in the majority of cells (64%), corresponding with the fact that ArlH is part of the archaellum motor (Figure 5b). Possibly, fusion of GFP to the C-terminus of ArlH, blocks interaction with other proteins or hinders its function, thus rendering this mutant non-motile.

Western blot analysis of the GFP-arlH fusion protein showed two bands, in size corresponding to ArlH and to GFP (Figure S1b). Thus, the GFP-ArlH fusion protein was likely cleaved. Fluorescence microscopy analysis suggested that this is indeed the case, as GFP-ArlH expression in a ΔarlH resulted in a diffuse GFP signal in the
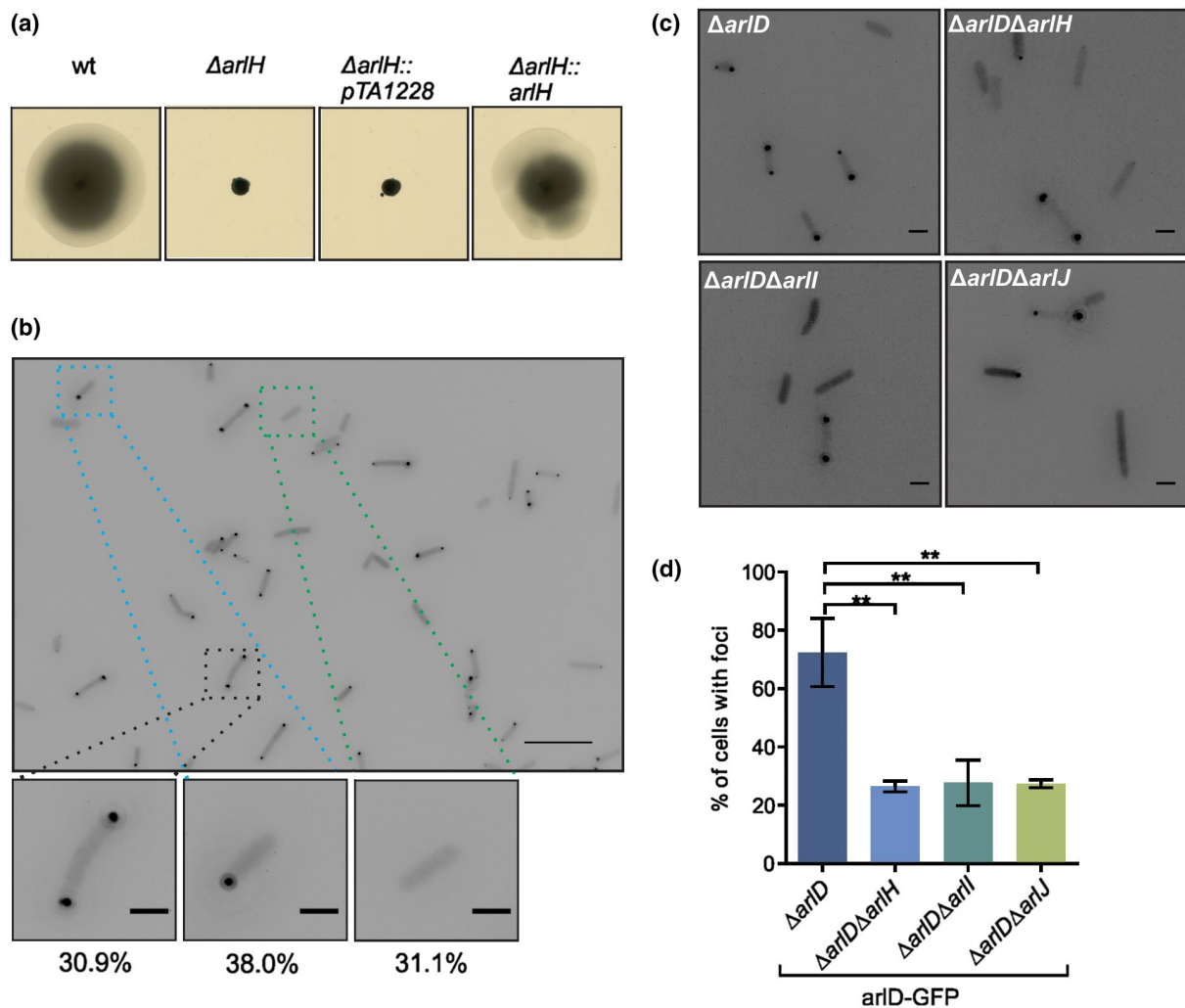

FIGURE 5 Polar localization of ArlD is mainly determined by binding to the archaellum motor (a) Influence of ArlH on directional movement. Motility assay on the semi-solid agar plate of different *H. volcanii* strains in rich medium. pTA1228, empty plasmid (b) Intracellular distribution of GFP-ArlH clusters in the *H. volcanii* ΔarlH strain. The percentage of total cells with each pattern is shown at the bottom. *n* > 500. Scale bars, 10 μm (upper panel) and 2 μm (lower panels). (c) Representative fluorescent images of intracellular distribution of ArlD-GFP *H. volcanii* strains in which different archaellum motor proteins were deleted. ΔarlD, ΔarlD ΔarlH, ΔarlD ΔarlI, ΔarlD ΔarlJ. The number of each analyzed mutant, *n* > 500. Scale bars, 2 μm. (d) Percentages of cells with intracellular ArlD-GFP foci in strains described in (c). **$p < .01$ as established by *t* test

cytoplasm (Figure 5b). GFP-ArlH could restore the motility of a Δ*arlH* strain on the semi-solid agar plate, which is likely the result of the incorporation of the cleaved ArlH, without GFP tag (Figure 5a), in the archaellum motor.

Next, the double deletion strains Δ*arlD* Δ*arlH* and Δ*arlCE* Δ*arlH* were constructed to test the influence of ArlH on ArlD and ArlCE positioning. The number of cells with polar foci was reduced significantly in the Δ*arlD* Δ*arlH* strain expressing ArlD-GFP (27%), in comparison with expression of this construct in the Δ*arlD* strain (69%) (Figure 5c,d). ArlD-GFP was correctly expressed in this background as observed by Western blot analysis (Figure S1c). A similar observation was made for ArlCE-GFP expression in the Δ*arlCE* Δ*arlH* strain, where a reduction of ~70% to ~36% of cells with polar foci was detected (Figure S4a,b). As the polar positioning of both ArlD and ArlCE was severely diminished in the absence of ArlH (Figures 5c,d, S4a,b), ArlD and ArlCE likely dock to the archaellum motor via ArlH. However, ~30% of cells still form ArlD-GFP or ArlCE-GFP foci at the cell pole in the Δ*arlH* strains (Figures 5c,d, S4a,b), which indicates that ArlD and ArlCE can also position themselves at the cell pole by another mechanism. To test if the remainder of polar localization of ArlD and ArlCE, might be caused by interaction with other archaellum motor proteins, we created knockouts of ArlI and ArlJ in *H. volcanii*. ArlI is in direct interaction with ArlH, while ArlJ a membrane protein to which ArlI is bound (Banerjee *et al.*, 2013; Chaudhury *et al.*, 2016). For this reason, ArlH is not expected to bind to the archaellum motor in the absence of either ArlI or ArlJ. Analysis on motility plate showed that the Δ*arlI* strain and Δ*arlJ* strain did not form motility rings (Figure S4c), which corresponds to the previously reported absence of archaella in similar knock-out strains in other archaea (Patenge *et al.*, 2001; Thomas *et al.*, 2002; Chaban *et al.*, 2007). Expression of GFP-ArlI in Δ*arlI* could restore the motile phenotype on the semi-solid agar plates (Table S1, Figure S4c). ArlI-GFP expression did not restore motility (Table S1). Expression of both fusion proteins was extremely low and could not be detected by Western blot analysis, while fluorescence microscopy showed a faint signal at the cell poles when GFP-ArlI was expressed in a Δ*arlI* background (Figure S4d).

Expression of ArlD-GFP in Δ*arlD* Δ*arlI* resulted in a reduction of the percentage of cells with polar foci (~28%) compared to the expression of the same construct in the Δ*arlD* strain (~70%) (Figure 5c). Similarly, when *arlJ* was deleted, 27% of cells kept polar ArlD-GFP foci. Thus, after the deletion of either *arlH*, *arlI*, and *arlJ* the number of cells with polar ArlD foci is strongly reduced but does not drop below 25%. Similar expression levels of ArlD-GFP were detected in all strains by Western blot analysis (Figure S1c). Comparable results were obtained for an ArlCE-GFP construct in a Δ*arlCE* Δ*arlH*, a Δ*arlCE* Δ*arlI* and a Δ*arlCE* Δ*arlJ* strain (Figure S4a,b). This suggests that positioning of ArlD and ArlCE at the cell poles, relies mainly on binding of these proteins to ArlH. However, a smaller population of ArlD and ArlCE proteins might also associate with unknown polar factors.

2.5 | Dynamics of ArlCE and ArlD

ArlD foci are dynamic in vivo and were previously shown to display mobility in the polar region of the cell (Li *et al.*, 2019) (Movie S1, Figure 6a). ArlD movement is mainly restricted to the cell pole, and occasionally also the movement from particular small ArlD foci was observed from one cell pole to another (Li *et al.*, 2019). As our above-described findings suggested that ArlCE and ArlD might form a precomplex required for interaction with the archaellum motor, we first made fluorescent time-lapse movies of ArlCE-GFP expressed in a *H. volcanii* Δ*arlCE* strain. Dynamic behavior of ArlCE was observed, specifically restricted to the cell pole (Figure 6b, Movie S2). This movement of ArlCE was largely similar to the behavior of ArlD. We assumed that this highly dynamic ArlD and ArlCE foci represent a part of the population that is not bound to the archaellum motor. To test this hypothesis, we studied the localization of the archaellum motor by time-lapse microscopy of a Δ*arlH* strain expressing ArlH-GFP. ArlH foci remained localized at the cell pole over the course of an hour, suggesting that the archaellum motor is stably positioned at the cell pole (Movie S3, Figure 6c). This behavior is different from that of the dynamic behavior of ArlD and ArlCE. Together with the above-described data, this suggests that ArlCE and ArlD likely form a complex, and that these complexes are localized at one or both cell poles. As the majority of the ArlCE and ArlD population is bound to the archaellum motor via ArlH, it is likely that specifically the
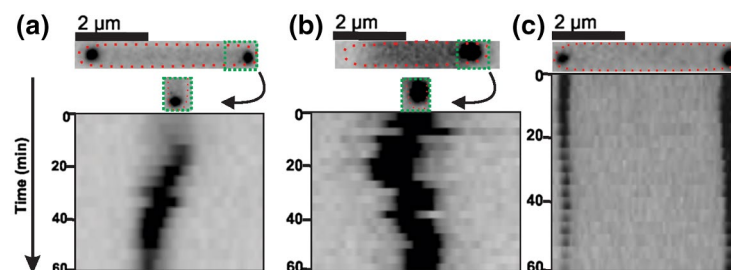
FIGURE 6 Intracellular dynamics of archaellum proteins ArlCE, ArlD, and ArlH. Time-lapse images of (a) Δ*arlD*:: ArlD-GFP (b), Δ*arlCE*:: ArlCE-GFP (c) and Δ*arlH*:: GFP-ArlH. The upper panel shows a fluorescent image of the selected cells in which GFP-fused proteins were followed for 60 min. The lower panel displays kymographs of the cells shown on top. Cells are representable for >20 analyzed cells per strain. See also Movies S1, S2, and S3

unbound ArlCE and ArlD populations display the dynamics in the polar region.

3 | DISCUSSION

The motility structures of bacteria and archaea have a fundamentally different structural organization. Yet, both receive input from the chemotaxis system. This system allows cells to direct their movement along chemical gradients in order to find optimal conditions for survival. In bacteria, the central response regulator CheY binds to proteins at the base of the flagellum motor, the "switch complex." As archaea lack homologs of the switch complex, we searched for archaellum motor proteins receiving signals from the chemotaxis system. Previously it has been shown that the archaeal-specific adaptor protein CheF is required for functional chemotaxis in archaea. This protein can bind to archaeal CheY. However, the sequence order in which chemotactic signals are transferred via CheY and CheF to the archaeal motility machinery was until now unresolved. Our findings suggest that the archaellum proteins ArlCE and ArlD are the direct receivers of signals from the chemotaxis system and represent the archaeal equivalent of the "switch complex."

By studying the localization of CheY-GFP fusions in different knock-out mutants, we could determine that in *H. volcanii*, CheY is primarily bound to the chemosensory arrays. This resembles the situation in *E. coli* where also the large majority of CheY proteins are present at the chemosensory arrays (Thiem *et al.*, 2007). In contrast, the polar positioning of CheF indicated that the largest fraction of this chemotaxis protein is normally bound to the archaellum motor.

Binding of CheF to the archaellum motor depends on the presence of both ArlCE and ArlD. Expression of fluorescent fusion proteins showed that ArlCE and ArlD co-localize and might form a complex. We suggest that the proteins form a precomplex, which is required for their binding to the archaellum motor. A strong interaction between these proteins would be in line with the fact that the *arlC*, *D*, and *E* genes in different combinations are often fused in archaellum operons of different euryarchaea (Chaban *et al.*, 2007; Jarrell and Albers, 2012). In addition, a dependency of these proteins on each other would fit well with the hypothesis that the ArlC, D, and E proteins make up the unassigned density at the base of the archaellum motor in the cryo-EM structures of euryarchaea (Briegel *et al.*, 2017; Daum *et al.*, 2017).

We found that the localization of both ArlCE and D depends on the archaellum motor protein ArlH (Figure 7). Also, this is in line with the hypothesis that ArlCDE make up the ring-like structure at the cytoplasmic side of the archaellum motor, since this part is in direct contact with the density in which the ArlH crystal structure could be mapped (Daum *et al.*, 2017).

Surprisingly a fraction of the ArlCE and ArlD proteins could still localize at the cell poles, even in absence of the archaellum motor (such as when ArlH, ArlI or ArlJ are deleted). Thus, ArlCE and ArlD are likely capable of binding to other unknown polar factors for their positioning. One candidate for this might be the "polar cap" or "cytoplasmic cone," which was revealed by whole-cell cryo-tomography of *P. furiosus* and

T. kodakaraensis at a defined distance below the archaella motors and the cell membrane (Briegel *et al.*, 2017; Daum *et al.*, 2017). The polar cap is likely a typical feature of motile euryarchaeal cells (Kupper *et al.*, 1994; Briegel *et al.*, 2017; Daum *et al.*, 2017). The polar cap is in close proximity to the archaellum motor, but a direct connection was not observed (Briegel *et al.*, 2017; Daum *et al.*, 2017). The protein constitution of this polar cap is not known. It might be possible that ArlCE and ArlD can interact with the unknown polar cap protein(s) and as such are polarly localized even in the absence of the archaellum. Precomplex formation might not be required for interaction with a pole organizing factor, as polar localization of GFP fused ArlD or ArlCE was still observed for a fraction of the cells, even when both *arlD* and *arlCE* were deleted. This is in contrast to the binding of ArlD and ArlCE to the archaellum motor, which is strongly impaired in the absence of either one of the proteins.

In summary, our findings suggest a central role for the ArlCE and ArlD proteins in the signal transduction from the chemotaxis system to the archaellum machinery. Extracellular stimuli are received by chemosensory receptors, organized in chemosensory arrays. Stimuli lead, via CheW, to the autophosporylation of CheA and phosphorylation of CheY (Figure 7). Phosphorylated CheY then interacts with the archaeal-specific chemotaxis protein CheF. CheF requires ArlCE and ArlD to bind to the archaellum motor. ArlCE and ArlD in turn rely on interaction with the central motor protein ArlH (Figure 7). Possibly, a small proportion of the ArlCE and ArlD proteins also interacts with a polar organizing factor, such as the polar cap (Figure 7). Euryarchaea encode ArlCDE encoded by euryarchaea. Crenarchaea do not possess a bacterial-like chemotaxis system and instead of ArCDE they encode ArlX.

Thus, for a functional interaction between the bacterial-like chemotaxis system and the archaeal motility machinery, two important features are required in those archaea possessing both systems: (a) the adaptor protein CheF and (b) ArlCDE that allow CheF binding to the archaellum motor. This work suggests that ArlCDE directly receive input from the chemotaxis system and might represent the archaeal equivalent of the switch complex. The hypothesis that they are conveniently located in the bell-like structure below the euryarchaeal archaellum motor, awaits further structural characterization of these three proteins.

4 | EXPERIMENTAL PROCEDURES

4.1 | Growth and genetic manipulation of *H. volcanii*

H. volcanii strains were cultured as previously described (Quax *et al.*, 2018b; Li *et al.*, 2019). Genetic manipulation and gene expression based on the selection with uracil in Δ*pyrE2* strains were performed with PEG 600 as described previously (Allers *et al.*, 2004). The cells were cultured at 45°C or 42°C, under constant rotation at 120 rpm, in complete YPC medium containing 5% Bacto™ yeast extract, 1% peptone (Oxoid, UK), 1% BactoTM Casamino acids (BD Biosciences, UK) or in selective CA medium containing only 5% BactoTM Casamino acids in 18% SW (Salt water, containing per liter
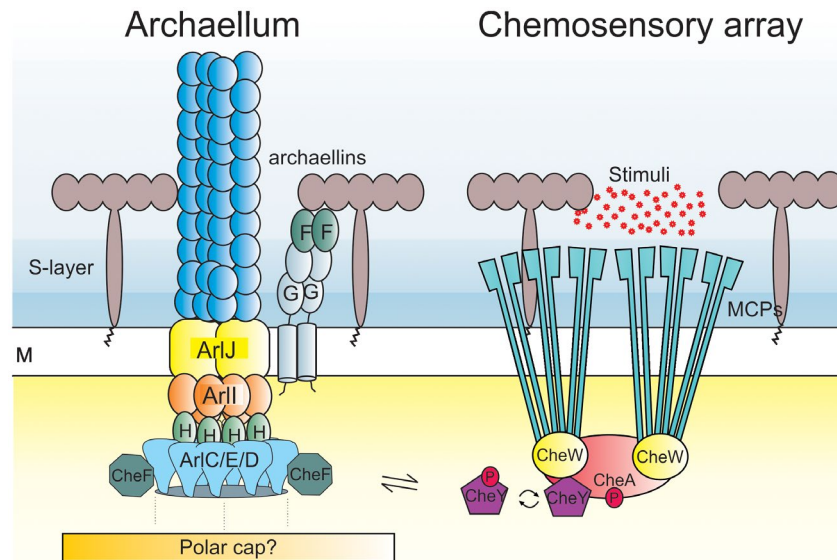
FIGURE 7 Simplified model of the chemotaxis signal transduction system and the archaellum in euryarchaea. MCPs are organized in chemosensory arrays together with CheW and CheA, which is necessary for signal integration and amplification. Autophosphorylation of CheA results in the phosphorylation of CheY. Phosphorylated CheY binds CheF, which is present at the base of the archaellum motor. CheF requires ArlCDE that form the switch complex, for binding to the archaellum motor. Possibly ArlCDE are not only binding to the archaellum motor protein ArlH, but are also interacting with the polar cap, to ensure polar localization. The individual proteins of the S-layer form a 2D crystal. Chemotaxis accessory proteins are left out for simplicity. Blue, extracellular environment. Yellow, cytoplasm. M, membrane. MCP, methyl-accepting chemotaxis protein. Red dots, environmental stimuli that bind to the MCPs

144 g NaCl, 21 g $MgSO_4$ X $7H_2O$, 18 g $MgCl_2$ X $6H_2O$, 4.2 g KCl, and 12 mM Tris HCl, pH 7.3). Plasmids based on pTA1228 (Brendel *et al.*, 2014), with *pyrE2* for selection with uracil, were constructed to express proteins in *H. volcanii* strains (Table S3). Plasmids based on pTA131 were used to create knock-out constructs for the pop-in pop-out method based on the pyrE2 gene. Salt stable GFP and mCherry genes were introduced to pTA1228 plasmid, allowing the expression of N-terminal and C-terminal fluorescent fusion proteins in *H. volcanii* strains (Duggin *et al.*, 2015).

4.2 | Deletions of genes in *H. volcanii* strains

The primers used to create knockout plasmids based on pTA131 are described in Table S2. Construction and transformation of knock-out plasmids were performed as described previously (Allers *et al.*, 2004). Selection for pop-in occurred on CA plates. This was followed by three transfers in liquid YPC medium. Then the inoculum was diluted 10^{-3} and cultured on CA plates with 50 µg/ml of 5-FOA and 10 µg/ml of uracil for the pop-out selection. Colonies were streaked on a new YPC plate, grown for two days, and subjected to a colony lift to Zeta-Probe® GT Blotting membranes (Biorad). After cell lysis and DNA cross-linking, the DNA was subjected to pre-hybridization and hybridization using a DIG High Prime DNA labeling and detection starter kit II (Roche) according to the manufacturer's instructions with a DIG-labeled probe of ~100-200 bp annealing in the targeted gene (for primer sequences, see Table S2). Colonies to which the probe did not bind were grown in liquid YPC media and genomic DNA was isolated as described previously (Allers *et al.*, 2004). The genomic DNA of several selected mutants was analyzed with PCR using primers that anneal outside of the flanking regions of the deleted gene (see Table S2) and the products formed were compared with those of the parent strain H26 on an agarose gel.

4.3 | Strains, plasmids, and primers

The strains, plasmid, and primer sequences used in this study is shown in Tables S2–S4.

4.3.1 | Motility assays of *H. volcanii* on semisolid agar plates

Motility assays were performed using the same method as previously described (Quax *et al.*, 2018b; Li *et al.*, 2019). Semi-solid agar plates were made in the YPC medium containing 0.3% agar, 50 µg/ml of uracil, and 1 mM tryptophan. Fresh cells were inoculated in 5 ml of CA medium with 50 µg/ml of uracil and/or tryptophan when required. About 10 µl of the inoculum of each strain was dropped on the same semi-solid agar plates. The experiment was performed at least three independent times (containing three biological replicates each). The motility ring formed after cultivation at 45°C for 5 days were scanned and the diameter was measured.

4.4 | Transmission electron microscopy

Cells were grown overnight at 42°C in CA medium to an OD600 of ~0.05 and then harvested by centrifugation at 3,000g for 10 min. Cells were concentrated and resuspended in CA medium with 2% (v/v) glutaraldehyde and 1% (v/v) paraformaldehyde. Cells were adsorbed to glow-discharged carbon-coated grids with Formvar films for 30 s. Samples were washed three times in distilled H_2O and negatively stained with 2% (w/v) uranyl acetate. Cells were imaged using a Philips CM10 transmission EM coupled to a Gatan BioScan camera and analyzed with Gatan DigitalMicrograph software.

4.5 | Western blotting

Strains were grown under similar conditions as those for fluorescence microscopy analysis. The cells were harvested by centrifugation and resuspended to a theoretical OD of 22. Total cell lysates were separated by SDS-PAGE (sodium dodecyl sulfate–polyacrylamide gel electrophoresis) on two 12% acrylamide gels. One gel was blotted to a PVDF (Polyvinylidene fluoride) membrane (Roche) by semi-dry Western blotting. The gels were stained with Quick Coomassie (Generon Ltd.). The membrane was subsequently incubated in blocking buffer (0.2% I-Block^{TM}, 0.1% Tween) (Thermo Fisher Scientific, MA, USA) at room temperature for 2 hr. After three times washing with PBST buffer (0.1 g/L of $CaCl_2$, 0.2 g/L of KCl, 0.2 g/L of KH_2PO_4, 0.1 g/L of $MgCl_2 \cdot 6H_2O$, 8 g/L of NaCl, 1.15 g/L of Na_2HPO_4, pH 7.4), the membrane was incubated with anti-GFP antibody diluted to 1:1,000 in PBST buffer for 1 hr at room temperature. After three washes in PBST, a secondary anti-rabbit antibody (from goat) coupled with HRP (horseradish peroxidase) (Thermo Fisher Scientific, MA, USA) was added to the membrane (1:5,000). Clarity ECL Western blotting substrate (Thermo Fisher Scientific) was used for the visualization of the chemiluminescent signals in a ECL ChemoCam Imager (Intas, Germany).

4.6 | Fluorescence microscopy

H. volcanii precultures were grown in 5 ml of CA medium overnight as described above. The next day the cultures were diluted to a theoretical OD of 0.005 in 20 ml of CA medium. After 16 hr incubation at 42°C (as described under "growth and genetic manipulation of *H. volcanii*"), the cultures had an OD of 0.01–0.05 and were imaged. During the last hour before observation by microscopy, 0.2 mM tryptophan was added. Cells were pipetted on an agarose pad (1% agar, 18% SW) and covered with a glass slip. The cells were observed at 100× magnification in the phase contrast (PH3) mode on a Zeiss Axio Observer 2.1 Microscope equipped with a heated XL-5 2000 Incubator running VisiVIEW® software. Each experiment was repeated on at least three independent occasions resulting in the analysis of over 500 cells per strain.

To track the mobility of protein foci with live imaging, 0.38% agar pads made of CA containing 1 mM tryptophan were poured in a round DF 0.17 mm microscopy dish (Bioptechs). After drying, the cells were placed underneath the agar pad, and the lid was placed on the microscopy dish. Images in the PH3 and GFP modes were captured at 100× magnification every 3 min for 1 hr at 45°C.

4.7 | Image analysis

Microscopy images were processed using the ImageJ plugin MicrobeJ (Ducret *et al.*, 2016). The number of foci per cell was counted and the cells were binned based on the number of cellular foci. The number of cells with the same positioning patterns was calculated as a percentage of the total. The same parameters for the detection of the fluorescent foci were used for all the proteins analyzed. Fluorescent foci movement in the time-lapse image series was characterized by time-space plots generated by the "Surface plotter" function in ImageJ (Ducret *et al.*, 2016). To determine if the percentage of cells with foci was significantly different between strains, an unpaired two-tailed t test was performed on the percentages calculated for each independent experiment (minimally 3). The total number of analyzed cells was >500 per strain.

CONFLICT OF INTEREST
The authors declare no conflict of interest.

AUTHOR CONTRIBUTIONS
T.E.F.Q. and S.-V.A. designed the research. Z.L., M.R., and T.E.F.Q. performed the research and interpreted the data. T.E.F.Q. and S.-V.A. wrote the paper. All authors read and contributed to the manuscript.

DATA AVAILABILITY STATEMENT
The data that supports the findings of this study are available in the supplementary material of this article.

ORCID
Sonja-Verena Albers https://orcid.org/0000-0003-2459-2226
Tessa E. F. Quax https://orcid.org/0000-0001-5516-5871

REFERENCES

Alam, M. and Oesterhelt, D. (1984) Morphology, function and isolation of halobacterial flagella. *Journal of Molecular Biology*, 176, 459–475.

Albers, S.-V. and Jarrell, K.F. (2015) The archaellum: how archaea swim. *Frontiers in Microbiology*, 6, 23.

Albers, S.-V. and Jarrell, K.F. (2018) The archaellum: an update on the unique archaeal motility structure. *Trends in Microbiology*, 26, 351–362.

Allers, T., Ngo, H.P., Mevarech, M. and Lloyd, R.G. (2004) Development of additional selectable markers for the halophilic archaeon *Haloferax volcanii* based on the leuB and trpA genes. *Applied and Environmental Microbiology*, 70, 943–953.

Altegoer, F. and Bange, G. (2015) Undiscovered regions on the molecular landscape of flagellar assembly. *Current Opinion in Microbiology*, 28, 98–105.

Banerjee, A., Neiner, T., Tripp, P. and Albers, S.V. (2013) Insights into subunit interactions in the *Sulfolobus acidocaldarius* archaellum cytoplasmic complex. *FEBS Journal*, 280, 6141–6149.

Barak, R. and Eisenbach, M. (1992) Correlation between phosphorylation of the chemotaxis protein CheY and its activity at the flagellar motor. *Biochemistry*, 31, 1821–1826.

Bardy, S.L. and Jarrell, K.F. (2003) Cleavage of preflagellins by an aspartic acid signal peptidase is essential for flagellation in the archaeon *Methanococcus voltae*. *Molecular Microbiology*, 50, 1339–1347.

Beeby, M., Ferreira, J.L., Tripp, P., Albers, S.-V. and Mitchell, D.R. (2020) Propulsive nanomachines: the convergent evolution of archaella, flagella, and cilia. *FEMS Microbiology Reviews*. [Epub ahead of print]. https://doi.org/10.1093/femsre/fuaa006

Berg, H.C. and Anderson, R.A. (1973) Bacteria swim by rotating their flagellar filaments. *Nature*, 245, 380–382.

Bi, S. and Sourjik, V. (2018) Stimulus sensing and signal processing in bacterial chemotaxis. *Current Opinion in Microbiology*, 45, 22–29.

Brendel, J., Stoll, B., Lange, S.J., Sharma, K., Lenz, C., Stachler, A.-E., et al. (2014) A complex of Cas proteins 5, 6, and 7 is required for the biogenesis and stability of clustered regularly interspaced short palindromic repeats (crispr)-derived rnas (crrnas) in *Haloferax volcanii*. *Journal of Biological Chemistry*, 289, 7164–7177.

Briegel, A., Ladinsky, M.S., Oikonomou, C., Jones, C.W., Harris, M.J., Fowler, D.J., et al. (2014) Structure of bacterial cytoplasmic chemoreceptor arrays and implications for chemotactic signaling. *eLife*, 3, e02151.

Briegel, A., Li, X., Bilwes, A.M., Hughes, K.T., Jensen, G.J. and Crane, B.R. (2012) Bacterial chemoreceptor arrays are hexagonally packed trimers of receptor dimers networked by rings of kinase and coupling proteins. *Proceedings of the National Academy of Sciences of the United States of America*, 109, 3766–3771.

Briegel, A., Oikonomou, C.M., Chang, Y.-W., Kjær, A., Huang, A.N., Kim, K.W., et al. (2017) Morphology of the archaellar motor and associated cytoplasmic cone in *Thermococcus kodakaraensis*. *EMBO Reports*, 18, 1660–1670.

Briegel, A., Ortega, D.R., Huang, A.N., Oikonomou, C.M., Gunsalus, R.P. and Jensen, G.J. (2015) Structural conservation of chemotaxis machinery across Archaea and Bacteria. *Environmental Microbiology Reports*, 7, 414–419.

Chaban, B., Ng, S.Y., Kanbe, M., Saltzman, I., Nimmo, G., Aizawa, S., et al. (2007) Systematic deletion analyses of the fla genes in the flagella operon identify several genes essential for proper assembly and function of flagella in the archaeon, *Methanococcus maripaludis*. *Molecular Microbiology*, 66, 596–609.

Chaudhury, P., van der Does, C. and Albers, S.-V. (2018) Characterization of the ATPase FlaI of the motor complex of the *Pyrococcus furiosus* archaellum and its interactions between the ATP-binding protein FlaH. *PeerJ*, 6, e4984.

Chaudhury, P., Neiner, T., D'Imprima, E., Banerjee, A., Reindl, S., Ghosh, A., et al. (2016) The nucleotide-dependent interaction of FlaH and FlaI is essential for assembly and function of the archaellum motor. *Molecular Microbiology*, 99, 674–685.

Chevance, F.F. and Hughes, K.T. (2008) Coordinating assembly of a bacterial macromolecular machine. *Nature Reviews Microbiology*, 6, 455–465.

Daum, B., Quax, T.E.F., Sachse, M., Mills, D.J., Reimann, J., Yildiz, Ö., et al. (2014) Self-assembly of the general membrane-remodeling protein PVAP into sevenfold virus-associated pyramids. *Proceedings of the National Academy of Sciences of the United States of America*, 111, 3829–3834.

Daum, B., Vonck, J., Bellack, A., Chaudhury, P., Reichelt, R., Albers, S.-V., et al. (2017) Structure and *in situ* organisation of the *Pyrococcus furiosus* archaellum machinery. *eLife*, 6, e27470.

Ducret, A., Quardokus, E.M. and Brun, Y.V. (2016) MicrobeJ, a tool for high throughput bacterial cell detection and quantitative analysis. *Nature Microbiology*, 1, 16077.

Duggin, I.G., Aylett, C.H.S., Walsh, J.C., Michie, K.A., Wang, Q., Turnbull, L., et al. (2015) CetZ tubulin-like proteins control archaeal cell shape. *Nature*, 519, 362–365.

Erhardt, M., Namba, K. and Hughes, K.T. (2010) Bacterial nanomachines: the flagellum and type III injectisome. *Cold Spring Harbor Perspectives in Biology*, 2, a000299.

Ghosh, A., Hartung, S., van der Does, C., Tainer, J.A. and Albers, S.-V. (2011) Archaeal flagellar ATPase motor shows ATP-dependent hexameric assembly and activity stimulation by specific lipid binding. *The Biochemical Journal*, 437, 43–52.

Griswold, I.J., Zhou, H., Matison, M., Swanson, R.V., McIntosh, L.P., Simon, M.I., et al. (2002) The solution structure and interactions of CheW from *Thermotoga maritima*. *Natural Structural Biology*, 9, 121–125.

Jarrell, K.F. and Albers, S.V. (2012) The archaellum: an old motility structure with a new name. *Trends in Microbiology*, 20, 307–312.

Kalmokoff, M.L. and Jarrell, K.F. (1991) Cloning and sequencing of a multigene family encoding the flagellins of *Methanococcus voltae*. *Journal of Bacteriology*, 173, 7113–7125.

Kupper, J., Marwan, W., Typke, D., Grünberg, H., Uwer, U., Gluch, M., et al. (1994) The flagellar bundle of *Halobacterium salinarium* is inserted into a distinct polar cap structure. *Journal of Bacteriology*, 176, 5184–5187.

Lassak, K., Neiner, T., Ghosh, A., Klingl, A., Wirth, R. and Albers, S.V. (2012) Molecular analysis of the crenarchaeal flagellum. *Molecular Microbiology*, 83, 110–124.

Li, X., Fleetwood, A.D., Bayas, C., Bilwes, A.M., Ortega, D.R., Falke, J.J., et al. (2013) The 3.2 Å resolution structure of a receptor: CheA:CheW signaling complex defines overlapping binding sites and key residue interactions within bacterial chemosensory arrays. *Biochemistry*, 52, 3852–3865.

Li, Z., Kinosita, Y., Rodriguez-Franco, M., Nußbaum, P., Braun, F., Delpech, F., et al. (2019) Positioning of the motility machinery in Halophilic Archaea. *mBio*, 10(3), e00377-19.

Marwan, W., Alam, M., and Oesterhelt, D. (1991) Rotation and switching of the flagellar motor assembly in *Halobacterium halobium*. *Journal of Bacteriology*, 173, 1971–1977.

Paithankar, K.S., Enderle, M., Wirthensohn, D.C., Miller, A., Schlesner, M., Pfeiffer, F., et al. (2019) Structure of the archaeal chemotaxis protein CheY in a domain-swapped dimeric conformation. *Acta Crystallographica Section F Structural Biology Communications*, 75, 576–585.

Parkinson, J.S., Hazelbauer, G.L. and Falke, J.J. (2015) Signaling and sensory adaptation in *Escherichia coli* chemoreceptors: 2015 update. *Trends in Microbiology*, 23, 257–266.

Patenge, N., Berendes, A., Engelhardt, H., Schuster, S.C. and Oesterhelt, D. (2001) The fla gene cluster is involved in the biogenesis of flagella in *Halobacterium salinarum*. *Molecular Microbiology*, 41, 653–663.

Paul, K., Brunstetter, D., Titen, S. and Blair, D.F. (2011) A molecular mechanism of direction switching in the flagellar motor of *Escherichia coli*. *Proceedings of the National Academy of Sciences of the United States of America*, 108, 17171–17176.

Pohlschroder, M., Pfeiffer, F., Schulze, S. and Abdul Halim, M.F. (2018) Archaeal cell surface biogenesis. *FEMS Microbiology Reviews*, 42, 694–717.

Porter, S.L., Wadhams, G.H. and Armitage, J.P. (2011) Signal processing in complex chemotaxis pathways. *Nature Reviews Microbiology*, 9, 153–165.

Quax, T.E.F., Albers, S.-V. and Pfeiffer, F. (2018a) Taxis in archaea. *Emerging Topics in Life Sciences*, 2, 535–546.

Quax, T.E.F., Altegoer, F., Rossi, F., Li, Z., Rodriguez-Franco, M., Kraus, F., *et al*. (2018b) Structure and function of the archaeal response regulator CheY. *Proceedings of the National Academy of Sciences of the United States of America*, 115, E1259–E1268.

Reindl, S., Ghosh, A., Williams, G.J., Lassak, K., Neiner, T., Henche, A.-L., *et al*. (2013) Insights into FlaI functions in archaeal motor assembly and motility from structures, conformations, and genetics. *Molecular Cell*, 49, 1069–1082.

Salah Ud-Din, A.I.M. and Roujeinikova, A. (2017) Methyl-accepting chemotaxis proteins: a core sensing element in prokaryotes and archaea. *Cellular and Molecular Life Sciences*, 74, 3293–3303.

Sarkar, M.K., Paul, K. and Blair, D. (2010) Chemotaxis signaling protein CheY binds to the rotor protein FliN to control the direction of flagellar rotation in *Escherichia coli*. *Proceedings of the National Academy of Sciences of the United States of America*, 107, 9370–9375.

Schlesner, M., Miller, A., Besir, H., Aivaliotis, M., Streif, J., Scheffer, B., *et al*. (2012) The protein interaction network of a taxis signal transduction system in a halophilic archaeon. *BMC Microbiology*, 12, 272.

Schlesner, M., Miller, A., Streif, S., Staudinger, W.F., Muller, J., Scheffer, B., *et al*. (2009) Identification of Archaea-specific chemotaxis proteins which interact with the flagellar apparatus. *BMC Microbiology*, 9, 56.

Sourjik, V. and Berg, H.C. (2002) Binding of the *Escherichia coli* response regulator CheY to its target measured in vivo by fluorescence resonance energy transfer. *Proceedings of the National Academy of Sciences of the United States of America*, 99, 12669–12674.

Staudinger, W. (2008) *Investigations on Flagellar Biogenesis, Motility and Signal Transduction of* Halobacterium salinarum. Munich: LMU München.

Streif, S., Staudinger, W.F., Marwan, W. and Oesterhelt, D. (2008) Flagellar rotation in the archaeon *Halobacterium salinarum* depends on ATP. *Journal of Molecular Biology*, 384, 1–8.

Szabo, Z., Albers, S.V. and Driessen, A.J. (2006) Active-site residues in the type IV prepilin peptidase homologue PibD from the archaeon *Sulfolobus solfataricus*. *Journal of Bacteriology*, 188, 1437–1443.

Szurmant, H. and Ordal, G.W. (2004) Diversity in chemotaxis mechanisms among the bacteria and archaea. *Microbiology and Molecular Biology Reviews*, 68, 301–319.

Thiem, S., Kentner, D. and Sourjik, V. (2007) Positioning of chemosensory clusters in *E. coli* and its relation to cell division. *EMBO Journal*, 26, 1615–1623.

Thomas, N.A. and Jarrell, K.F. (2001) Characterization of flagellum gene families of methanogenic archaea and localization of novel flagellum accessory proteins. *Journal of Bacteriology*, 183, 7154–7164.

Thomas, N.A., Mueller, S., Klein, A. and Jarrell, K.F. (2002) Mutants in flaI and flaJ of the archaeon *Methanococcus voltae* are deficient in flagellum assembly. *Molecular Microbiology*, 46, 879–887.

Welch, M., Oosawa, K., Aizawa, S. and Eisenbach, M. (1993) Phosphorylation-dependent binding of a signal molecule to the flagellar switch of bacteria. *Proceedings of the National Academy of Sciences of the United States of America*, 90, 8787–8791.

Wuichet, K., Cantwell, B.J. and Zhulin, I.B. (2010) Evolution and phyletic distribution of two-component signal transduction systems. *Current Opinion in Microbiology*, 13, 219–225.

Wuichet, K. and Zhulin, I.B. (2010) Origins and diversification of a complex signal transduction system in prokaryotes. *Science Signalling*, 3, ra50.

SUPPORTING INFORMATION

Additional Supporting Information may be found online in the Supporting Information section.